Signatures of anisotropic diffusion around PeVatrons in 100 TeV gamma-ray data

G. Giacinti[1,2,3] T. Abounnasr[4] A. Neronov,[5,6] and D. Semikoz[5]

[1]*Tsung-Dao Lee Institute, Shanghai Jiao Tong University, Shanghai 201210, People's Republic of China*
[2]*School of Physics and Astronomy, Shanghai Jiao Tong University, Shanghai 200240, People's Republic of China*
[3]*Max-Planck-Institut für Kernphysik, Postfach 103980, 69029 Heidelberg, Germany*
[4]*Institute for Cosmic Ray Research, The University of Tokyo, 5-1-5 Kashiwanoha, Kashiwa, Chiba 277-8582, Japan*
[5]*Université de Paris Cite, CNRS, Astroparticule et Cosmologie, F-75013 Paris, France*
[6]*Laboratory of Astrophysics, Ecole Polytechnique Federale de Lausanne, CH-1015 Lausanne, Switzerland*

The Tibet ASγ collaboration has reported a diffuse γ-ray emission signal from the Galactic Plane. We consider the possibility that the diffuse emission from the outer Galactic Plane at the highest energies is produced by cosmic rays spreading from a single supernova-type source either in the Local or Perseus arm of the Milky Way. We show that anisotropic diffusion of multi-PeV cosmic rays along the Galactic magnetic field can produce an extended source spanning ten(s) of degrees on the sky, with a flux-per-unit-solid-angle consistent with Tibet ASγ measurements. Observations of this new type of very extended sources, and measurements of their morphologies, can be used to characterize the anisotropic diffusion of PeV cosmic rays in the Galactic magnetic field, and to constrain the locations and properties of past PeVatrons.

I. INTRODUCTION

The detections of diffuse γ-ray emission from the Galactic Plane by Tibet ASγ experiment [1], and of isolated γ-ray sources by HAWC [2] and LHAASO [3] have extended the energy frontier of astronomy into the previously unexplored Peta-electronvolt energy range. Charged particles, possibly protons and nuclei, producing PeV γ-rays have energies in the ~ 10 PeV energy range, i.e., in the range of the "knee" of the cosmic ray spectrum [4,5]. The two types of γ-ray signals: diffuse emission and fluxes from isolated sources, are certainly related to each other. Isolated sources inject multi-PeV cosmic rays with a yet-to-be-determined spectrum into the interstellar medium, while the propagation of these cosmic rays through the interstellar medium generates the diffuse γ-ray flux.

The details of the relation between the properties of isolated sources of PeV cosmic rays, called "PeVatrons," and the properties of the cosmic ray spectrum in the

interstellar medium are not clear. Isolated sources detected by HAWC and LHAASO typically have rather soft spectra $dN_\gamma/dE \propto E^{-\Gamma_\gamma}$ with slopes $\Gamma_\gamma \geq 3$ in the 0.1–1 PeV energy range. On the one hand, the assumption that the gamma-ray spectra are the product of the p-p interactions of cosmic rays injected from these sources with the ISM leads to $\Gamma_{\rm inj} \sim \Gamma_\gamma$ in the PeV range, where $\Gamma_{\rm inj}$ is the slope of the cosmic rays injected by the source, so that the spectra of these should also be softer than E^{-3}, if one assumes that the spectrum of the escaped cosmic rays reflects that of the accelerated particles. On the other hand, considering that the cosmic ray spectrum observed at earth, with slope, $\Gamma_{\rm loc} \sim 3 > 2.5$ is already soften by the diffusive escape of PeV cosmic rays from the Galactic cosmic ray halo implies that the active hadronic sources should be harder than $E^{-2.5}$. In this situation, it is difficult to reconcile the LHASSO observation of a soft-spectrum source population with local measurements. The solution to this puzzle may lie in the peculiarities of the escape of very-high-energy cosmic rays from their sources and/or of the propagation of multi-PeV cosmic rays in the Galactic magnetic field. Another possibility is that the PeVatrons observed by LHASSO are leptonic sources powered by pulsars, in which case the suppression by Klein-Nishina effect of the Inverse Compton emission at energies above 10 TeV provides a natural explanation for the soft spectrum [6] while some

other hadronic sources could be the one contributing to the local spectrum.

Understanding the processes of cosmic ray escape from their sources and of cosmic ray propagation through the interstellar medium may be facilitated if the γ-ray emission from "clouds" of escaped cosmic rays could be reliably identified around individual sources. This is perhaps difficult in the GeV-to-TeV energy range where sources are numerous and diffusion of cosmic rays through the interstellar medium is slow. In this case, the extended γ-ray emission produced by cosmic rays spreading from individual sources may be difficult to trace on top of the much stronger collective diffuse emission produced by the entire source population [7]. However, the number of sources capable of accelerating particles to much higher energies is lower, and cosmic ray diffusion is faster for higher energy particles. In these conditions, the diffuse γ-ray emission in the highest, $\sim$PeV, energy range may be dominated by the signal from cosmic rays spreading from just a few sources. In this case, the identification of the extended emission from cosmic rays spreading from an individual source and the study of the morphology of the diffuse emission signal may clarify the details of the processes of injection of cosmic rays from the source and of cosmic ray propagation through the interstellar medium.

In the following, we explore if the hypothesis of superposition of diffuse emission from cosmic rays spreading from just a few single source(s) may explain the diffuse emission signal from the direction of outer Galactic Plane observed by Tibet ASγ. We model the evolution of the distribution of cosmic rays spreading from a single source through the ordered and turbulent Galactic magnetic fields, using a Monte-Carlo technique tracing individual trajectories of cosmic rays. We calculate the γ-ray signal from the decays of neutral pions produced by interactions of cosmic rays spreading around the source and compare the predicted morphology of the γ-ray signal with the Tibet ASγ data.

II. POSSIBLE SOURCE LOCATIONS IN THE OUTER MILKY WAY DISK

To determine the most likely locations for individual PeVatrons in the outer Galaxy, we briefly review in this section the structure of the Milky Way disk and outline the model we use in the calculations of the subsequent sections. The Milky Way is a four-armed barred spiral galaxy [8,9]. The Sun is located at the distance $D_\odot = 8.15 \pm 0.15$ kpc [10] from the Galactic Center, in the immediate vicinity of the Orion—or "Local"—arm, which lies between the Sun and the Perseus arm, see Fig. 1.

An analytical model for the spiral arm structure can be defined as in Ref. [10]:

$$r(\theta) = R_0 \exp\left[\tan(p)(\theta - \theta_0)\right], \qquad (1)$$
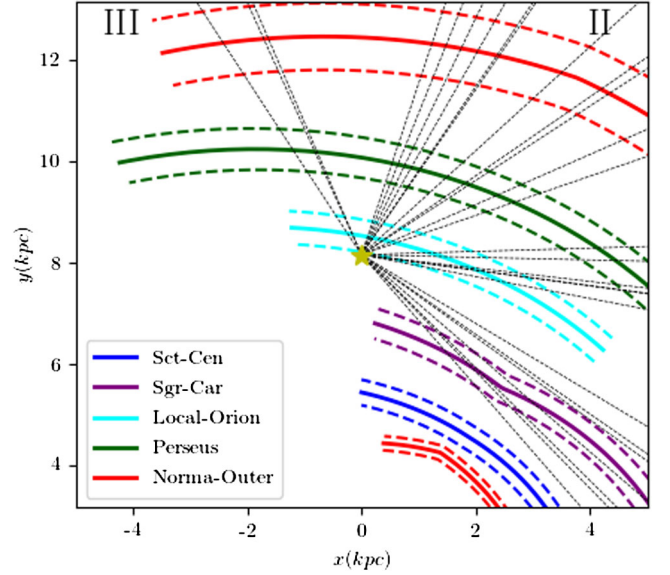

FIG. 1. Milky Way spiral arm structure as defined in Ref. [10], and zoomed-in around the Sun's position (yellow star). The dotted lines represent the directions (projected onto the Galactic plane) of the 398–1000 TeV Tibet ASγ events from [1] with $|b| < 15°$.

where (r and θ) denote the polar coordinates in the Galactic disk, and R_0, θ_0, and p are parameters defined differently for the Perseus, Norma, Scrutum, and Sagittarius arms. Following Ref. [10], we use two different values for the pitch angles p of each arm. The arm structure and their scale widths can be found in Table 2 of [10]. We plot this spiral arm structure in Fig. 1, where the dashed lines correspond to the scale widths of the arms.

For the gas density in the interstellar medium, we adopt a simple model loosely based on the model presented in Ref. [11]. In each spiral arm, we assume that the gas number density follows:

$$n_{\text{ism}} = n_{\text{arm},0} \exp\left(-\frac{z^2}{2\sigma_z^2}\right), \qquad (2)$$

where $n_{\text{arm},0}$ is the mid-plane density for each arm, and z is the distance to the Galactic plane. The vertical scale height of the arms $\sqrt{2}\sigma_z$ is chosen such that:

$$\sigma_z = \begin{cases} 40 \text{ pc}, & r < 7 \text{ kpc} \\ 40 \text{ pc} + 72 \frac{\text{pc}}{\text{kpc}}(r - 7 \text{ kpc}), & r \geq 7 \text{ kpc}, \end{cases} \qquad (3)$$

which is twice the rms value evaluated in [10].

The Galactic disk has a warp that can be described as a shift of the middle plane along the z axis. We include this warp in our calculations, using the formula provided in Eq. (1) of Ref. [12]. Viewed from the Sun's position, the presence of this warp leads to a slight shift of the galactic
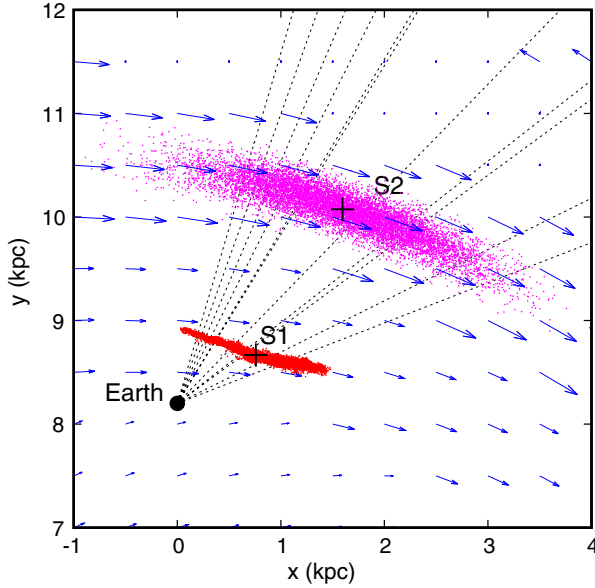
FIG. 2. Sketch of a 5 kpc × 5 kpc region of interest of the Galactic plane, seen from above. The black dot represents the Earth's location, and the two black crosses are those of "S1" (Source in the local—Orion—arm) and "S2" (Source in the Perseus arm). The red and magenta dots represent the locations, projected onto the Galactic plane, of the 10^4 simulated cosmic rays that have escaped respectively from S1 and from S2. The blue arrows show the directions of the regular Galactic magnetic field in the (x-y) plane at $z = 0$ in the Jansson and Farrar model [13,14], and their sizes are proportional to the field strength. The thin black dotted lines represent the directions (projected onto the Galactic plane) of the 11 Tibet ASγ events at $l \approx 110°$–$170°$ and $|b| < 15°$. The choice for the locations of the S1 and S2 along their respective spiral arm (i.e., toroidal direction) is qualitative, roughly chosen in the middle of the 11 projected directions.

plane not larger than 2°, and it only has a small effect in the region of the Galactic disk that we consider in Sec. IV.

For the regular and turbulent components of the Galactic magnetic field, we adopt the Jansson and Farrar model from Refs. [13,14], with a rescaling of the strength of its turbulent component as explained in Sec. IV. In the Galactic disk, at $z = 0$, the regular magnetic field is almost aligned with the spiral arm structure. In Fig. 2, we plot with blue arrows the direction and strength of this regular magnetic field at $z = 0$. One can see that it follows globally the directions of the Local and Perseus arms from Fig. 1.

In Fig. 1, we show with dotted black lines the directions of the Tibet ASγ events from [1], that are in the 398–1000 TeV energy range and lie at Galactic latitudes $|b| < 15°$. These events likely correspond to the diffuse γ-ray emission from the Galactic plane. In Fig. 2, we only plot the directions of the 11 events that lie at $l = 110°$–$170°$. One can clearly see that a multi-PeV cosmic ray source located in either the Local arm or the

Perseus arm could in principle inject particles that would diffuse along the magnetic field in these arms and produce some of these 11 events. In the following two sections, we investigate analytically and numerically if such a scenario is viable.

III. PROPAGATION OF COSMIC RAYS FROM A SOURCE IN THE LOCAL AND PERSEUS ARMS AND DIFFUSE γ-RAY EMISSION

Cosmic rays spiral along magnetic field lines and are scattered by the turbulent component of the Galactic magnetic field. In a simple *leaky box* model, cosmic rays escape out of the galactic disk diffusively, the components of the diffusion tensor depending on the angle ϑ of the regular magnetic field B_{reg} with the galactic plane and the strength of isotropic turbulence B_{rms}. It was shown in [14] that a low level of turbulence $B_{\mathrm{rms}}/B_{\mathrm{reg}} < 1$ is required to accommodate Boron-to-Carbon ratio measurements over a wide range of (reasonable) parameters, so that the total magnetic field $B_{\mathrm{tot}} = B_{\mathrm{reg}} + B_{\mathrm{rms}}$ must have a definite mean direction. Diffusion of particles in superimposed regular and turbulent magnetic fields is therefore anisotropic with different diffusion coefficients $D_{\parallel}$, $D_{\perp}$ parallel and perpendicular to the regular magnetic field direction. Both diffusion coefficients scale as a power law in energy $D_{\parallel} \propto E_p^{\delta_{\parallel}}$, $D_{\perp} \propto E_p^{\delta_{\perp}}$ and numerical modeling indicates that $\delta_{\parallel} \simeq \delta_{\perp}$, so that we drop the indexes $\parallel$, $\perp$ for δ [15]. The assumption of turbulence with a Kolmogorov spectrum fixes δ to the value $\delta = 1/3$. Numerically propagating individual cosmic rays in synthetic Kolmogorov turbulence, we find that [15]

$$D_{\perp} \simeq 10^{28} \left[\frac{E_p}{1\ \mathrm{PeV}}\right]^{\delta}\ \mathrm{cm^2/s}$$

$$D_{\parallel} \simeq 10^{31} \left[\frac{E_p}{1\ \mathrm{PeV}}\right]^{\delta}\ \mathrm{cm^2/s} \qquad (4)$$

for our choice of parameters of magnetic field with the root-mean-square of the turbulent component and the regular field strength related as $B_{\mathrm{rms}}/B_{\mathrm{reg}} = 0.5$. This value represents a minimally anisotropic case where the ordered magnetic field is completely perpendicular to the galactic plane while the level of isotropic turbulence with realistic, smaller angle, would require to decrease the level of turbulence hence increasing anisotropy. It has to be noted that the diffusive propagation of cosmic rays in the turbulent magnetic field is ensured by resonant scattering occurring at gyroradii

$$R_L = \frac{E_p}{eB} \sim 3 \left[\frac{E_p}{10\ \mathrm{PeV}}\right] \left[\frac{B}{3\ \mu\mathrm{G}}\right]^{-1}\ \mathrm{pc} \qquad (5)$$

smaller than the inverse resonant wave number $k_{res}^{-1} = \frac{L_{coh}}{2\pi}$, that is

$$R_L < \frac{1}{k_{res}} = \frac{L_{coh}}{2\pi} \simeq 4 \left[\frac{L_{max}}{100 \text{ pc}} \right] \text{ pc.}$$

Where the coherence length of the turbulent magnetic field is related to the maximum scale of fluctuations by $L_{coh} = L_{max}/5$ in the case of Kolmogorov turbulence [15]. Considering the maximum scale of the turbulence to be $L_{max} \sim 10^2$ pc guarantees that cosmic rays with energies up to 10 PeV (producing sub-PeV γ-ray emission in interactions with the interstellar medium) can propagate in the ISM in the diffusive regime.

Cosmic rays released from a source T_s years ago spread to the distance

$$d_\parallel \sim \sqrt{D_\parallel T_s} \simeq 1 \left[\frac{T_s}{10 \text{ kyr}} \right]^{1/2} \left[\frac{E_p}{10 \text{ PeV}} \right]^{1/6} \text{ kpc}$$

$$d_\perp \sim \sqrt{D_\perp T_s} \simeq 30 \left[\frac{T_s}{10 \text{ kyr}} \right]^{1/2} \left[\frac{E_p}{10 \text{ PeV}} \right]^{1/6} \text{ pc} \quad (6)$$

Cosmic rays contained in such ellipsoid-shaped regions (of dimensions $2d_\parallel \times 2d_\perp \times 2d_\perp$) form an extended overdensity on top of the average "sea" of cosmic rays from multiple sources accumulated on the timescale of escape from the Galactic disk. This timescale is long for cosmic rays with relatively low (GeV) energy, so that the overdensity created by a single source is difficult to spot. The shortening of the escape timescale with increasing cosmic ray energy leads to a lower level of the cosmic ray "sea" and a stronger overdensity due to a single source.

It is possible to detect the ellipsoid-shaped overdensity of cosmic rays around a single source through the γ-ray and neutrino emission that it produces through interactions of cosmic rays with the interstellar medium. Multi-PeV cosmic rays produce γ-rays with energies $E_\gamma \simeq 0.1 E_p$. As an example, the γ-ray emission from a region of projected size $2d_\parallel \times 2d_\perp$ around a source situated at the distance $d_s \sim 2$ kpc in the Perseus arm is expected to span a region of angular size $\Delta_{\parallel,\perp} = 2d_{\parallel,\perp}/d_s$,

$$\Delta_\parallel \simeq 60° \left[\frac{T_s}{10 \text{ kyr}} \right]^{1/2} \left[\frac{E_\gamma}{0.1 \text{ PeV}} \right]^{1/6} \left[\frac{d_s}{2 \text{ kpc}} \right]^{-1}$$

$$\Delta_\perp \simeq 2° \left[\frac{T_s}{10 \text{ kyr}} \right]^{1/2} \left[\frac{E_\gamma}{0.1 \text{ PeV}} \right]^{1/6} \left[\frac{d_s}{2 \text{ kpc}} \right]^{-1}, \quad (7)$$

which can thus occupy a sizeable part of the Galactic Plane observed by Tibet ASγ.

Cosmic rays lose energy in interactions with ambient gas on the timescale

$$t_{pp} = (c\sigma_{pp} n_{ism})^{-1} \simeq 3 \times 10^7 \left[\frac{n_{ism}}{1 \text{ cm}^{-3}} \right]^{-1} \text{ yr,} \quad (8)$$

where $\sigma_{pp} \simeq 3 \times 10^{-26}$ cm^2 is the pp interaction cross-section and n_{ism} is the density of the interstellar medium. These interactions produce the γ-ray luminosity

$$L_\gamma = \frac{\kappa E_p (d\mathcal{E}_s/dE_p)}{t_{pp}}$$

$$\simeq 10^{34} \left[\frac{\kappa}{0.1} \right] \left[\frac{E_p (d\mathcal{E}_s/dE_p)}{10^{49} \text{ erg}} \right] \left[\frac{n_{ism}}{1 \text{ cm}^{-3}} \right] \text{ erg/s,} \quad (9)$$

where $E_p (d\mathcal{E}_s/dE_p) \equiv E_p^{tot}$ is the total energy of cosmic rays injected by the source in the (decade wide) PeV energy range and κ is the fraction of the cosmic ray energy transferred to γ-rays in each interaction. Considering a SNR-like source with $E_{tot} \sim 10^{51}$ erg. If it converts 10% of it energy into cosmic rays and about another 10% of the energy budget remaining in the 1–10 PeV range for a spectrum $\frac{dN_{CR}}{dE_{CR}} \propto E^{-2}$, it accounts for 10^{49} erg of CR energy converted into γ-ray.

The flux from a source at a distance d_s is

$$F_\gamma = \frac{L_\gamma}{4\pi d_s^2}$$

$$\simeq 10^{-9} \left[\frac{\kappa}{0.1} \right] \left[\frac{E_p^{tot}}{10^{49} \text{ erg}} \right] \left[\frac{n_{ism}}{1 \text{ cm}^{-3}} \right] \left[\frac{d_s}{2 \text{ kpc}} \right]^{-2} \frac{\text{GeV}}{\text{cm}^2 \text{ s}} \quad (10)$$

The flux per unit solid angle is

$$\frac{dF_\gamma}{d\Omega} = F_\gamma \cdot \frac{d_s^2}{(2d_\parallel \times 2d_\perp)}$$

$$\simeq 3 \times 10^{-7} \left[\frac{\kappa}{0.1} \right] \left[\frac{E_p^{tot}}{10^{49} \text{ erg}} \right] \left[\frac{n_{ism}}{1 \text{ cm}^{-3}} \right] \left[\frac{T_s}{10 \text{ kyr}} \right]^{-1}$$

$$\times \left[\frac{E_\gamma}{0.1 \text{ PeV}} \right]^{-1/3} \frac{\text{GeV}}{\text{cm}^2 \text{s sr}} \quad (11)$$

One can notice that the flux per unit solid angle does not depend on the source distance. Further away sources produce a smaller overall flux, but span a smaller solid angle on the sky, so that the surface brightness remains the same.

Comparing the estimate (11) with the diffuse emission flux measured by Tibet ASγ [1], we find that the contribution from a single source, in which the overall energy injection in cosmic rays was comparable to that expected for a supernova, can explain the observed flux-per-solid angle in different parts of the Galactic Plane. The PeV energy range is unique in this respect: elongated cosmic ray "bubbles" produced by anisotropic diffusion of cosmic rays from individual sources are expected to produce a γ-ray flux comparable to the overall diffuse emission flux.

At lower energies, the flux from individual elongated bubbles is the same as in the PeV band (assuming that individual sources inject cosmic rays with power law spectra with E^{-2} slope), but the overall level of diffuse emission (which is known to have a spectrum $\sim E^{-2.5}$ or softer [16–18]) is much higher than the single source flux.

IV. NUMERICAL MODELING

We confirm here the analytical estimates of the previous section with a numerical model based on the approach developed in Refs. [19,20]. It is a Monte-Carlo modeling based on the direct integration of the equations of motion of cosmic rays in Galactic magnetic field models. We demonstrate that at least 7 of the 11 events of Tibet ASγ in the region ($l \approx 110°–170°$, $|b| < 15°$) may have been produced by one former PeVatron located in the Local or Perseus arm.

We use the Jansson and Farrar model of [13,14], and the turbulent magnetic field is generated using the nested grid method from Ref. [21]. The turbulence is of Kolmogorov type with $L_{\max} = 150$ pc, i.e., $L_c = 30$ pc. Following our earlier findings in Refs. [19,20], we reduce the strength of the turbulent field, $B_{\rm rms}$, by a factor $1/5$ compared to the values quoted in [14], so as to fit the Boron-to-Carbon ratio. The original values of $B_{\rm rms}$ from Ref. [14] leading to a too large grammage and thereby to an overproduction of secondary nuclei.

We calculate the trajectories of 10^4 cosmic rays injected in random directions from a point source and save the positions of these particles at fixed times after the injection instant. We use such fixed time snapshots to estimate the density of cosmic rays in a region around the source position. We then use this density estimate to calculate the γ-ray emission from cosmic ray interactions with the interstellar medium, using the AAFrag numerical code [22,23]. The density of the target gas is given by Eqs. (2) and (3).

We consider two different source locations: a young nearby source located in the local Orion arm, which we denote as "S1" in the following, and a more distant, older source located in the Perseus arm, which we denote as "S2". The source S1 is located at $(x, y, z) = (0.758$ kpc, 8.67 kpc, $0)$ in the coordinate system of Figs. 1 and 2. Its age is $t = 3$ kyr. The source S2 is located at $(x, y, z) = (1.60$ kpc, 10.1 kpc, -250 pc) and its age is $t = 30$ kyr. We need S2 to be located at such a distance below the Galactic plane to fit the Tibet ASγ data. While this distance might seem large, it is reasonable and justified in view of the presence of high-mass stars at such distances from the Galactic plane in the Perseus arm: See the location of the black dots below the Galactic plane in the upper panel of Fig. 5 in Ref. [10].

Figure 2 shows a scatter plot of locations of the cosmic rays injected by each source 3 and 30 kyr after the injection moment. One can see that, consistently with the estimates of the previous section, the regions occupied by the cosmic
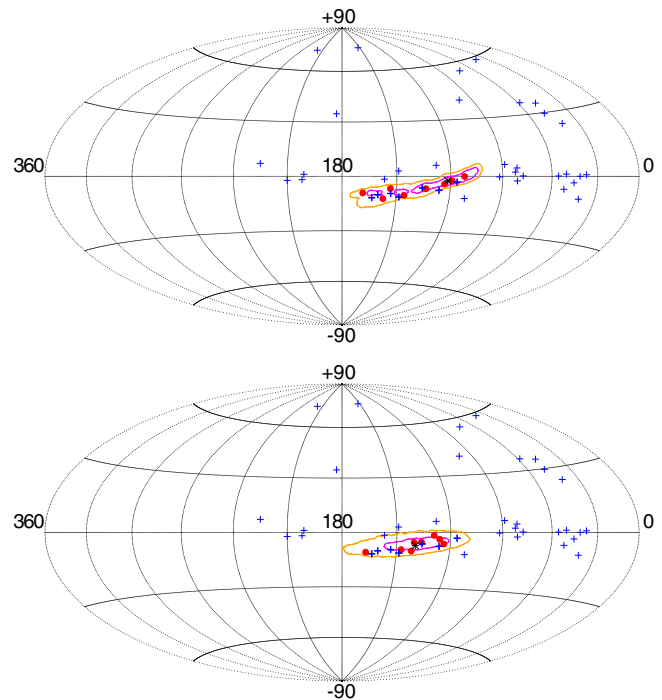

FIG. 3. Sky maps in Galactic coordinates showing the γ-ray emission in the 398–1000 TeV band produced by the cosmic rays that escaped from S1 (upper panel) and S2 (lower panel). The black stars show the locations of S1 and S2 on the sky. The magenta and orange contours encircle the regions with the largest surface brightness, containing respectively 50% and 95% of the total γ-ray emission. The red dots show simulated random sets of gamma-ray events that would be detected in the 398–1000 TeV energy range by a detector with Tibet ASγ's exposure [1]. The blue crosses represent the 38 Tibet ASγ events in the 398–1000 TeV energy range from Ref. [1]. The 7 Tibet ASγ events represented with thicker lines show the events falling within the source extensions.

rays are ellipsoids elongated in the direction of the ordered magnetic field in the Local and Perseus arms, respectively.

Figure 3 shows the maps of the 398–1000 TeV γ-ray emission resulting from the interaction of these cosmic rays with the gas in the interstellar medium (upper panel for S1, lower panel for S2). The contours correspond to the 50% and 95% signal containment. The arrival directions of the 38 Tibet ASγ events with 398–1000 TeV energies from Ref. [1] are represented with blue crosses. There are 7 aligned events in the region $l \approx 110°–170°$ and $-12° < b < 0$ (represented with thick blue crosses), which are all located within the 95% signal containment contours, both for S1 and for S2. To compare our predicted γ-ray signal with the Tibet ASγ dataset, we simulate the γ-ray events statistics that would be observed with the exposure and observation time reported for this experiment in [1]. Assuming that each source produces cosmic rays with an E^{-2} spectrum and with a total energy $E_{\rm CR}$ between 1 GeV and 10 PeV, we reproduce the correct event statistics, namely $\simeq 7 \pm 3$ photons in this energy

range, for a mid-plane gas density $n_{arm,0} \simeq 0.33((10^{50} \text{ erg})/E_{CR}) \text{ cm}^{-3}$ in the Local arm (S1), and $n_{arm,0} \simeq 1.5((3 \times 10^{50} \text{ erg})/E_{CR}) \text{ cm}^{-3}$ in the Perseus arm (S2). The simulated events are shown with the red dots in Fig. 3, for these values of target gas density. There are 8 events in both panels for the simulations shown here. The γ-ray event statistics predicted by our model is therefore consistent with that observed by Tibet ASγ, for the suggested source locations, and for standard midplane gas densities ($\sim 1 \text{ cm}^{-3}$) and typical supernova energies ($\sim 10^{51}$ erg in kinetic energy, out of which $\approx 10\%$ is channeled into cosmic rays). This demonstrates that these 7 aligned events in the data of Tibet ASγ can be explained by one same cosmic ray source, located either in our local arm or in the Perseus arm, and with an energy compatible of that of a single supernova.

For other sources locations, between those of S1 and S2, the shape of the γ-ray emission may slightly change, but would still keep such an elongated shape. It is therefore possible that one or a few of the other four nearby Tibet ASγ events at $l \approx 110°$–$170°$ and $|b| < 15°$ could be explained by the same source as the other seven events.

V. DISCUSSION AND CONCLUSION

Our calculations demonstrate that it is possible that the PeV-band diffuse emission from the Milky Way detected by Tibet ASγ may come from just several individual very extended sources. Such sources are formed by cosmic rays spreading from the points of injection (for example, by individual recent supernovae) preferentially along the ordered, kpc-scale Galactic magnetic field. The existence of such a new class of very extended sources can be verified with higher-statistics observations of the PeV diffuse emission by the LHAASO Observatory [24,25] that will be able to map the diffuse γ-ray flux from both the Galactic disk and regions at higher Galactic latitudes in the near future.

In the previous section, we focused on the Tibet ASγ events located in the region $l \approx 110°$–$170°$ of the Galactic plane. We note that our model may also provide an explanation for the other two bundles of events in the $l \approx 60°$–$110°$ region at $|b| < 15°$. Two compact spots

centered around $l \simeq 45°$ and $l \simeq 85°$ in the Galactic plane are clearly visible in Fig. 3. By comparing in Fig. 1 the arrival directions of these events (see the corresponding black dotted lines) to the Galactic spiral arm structure, one can see that the spots centered around $l \simeq 45°$ and $l \simeq 85°$ correspond, respectively, to the tangential directions to the Sagittarius arm and to the Local arm. Therefore, these two spots could be caused by one, or a few, extended sources in these arms. The fact that the regular Galactic magnetic field in these arms points approximately toward the Earth in these regions of the sky would explain why these spots appear more compact and less elongated than the source studied in Sec. IV: Their cosmic ray distributions would be more elongated along the line-of-sight, than across the sky. Comparison with future neutrino measurements will allow us to further constrain the origin of the gamma-ray emission, see, e.g., Ref. [26].

Finding candidates for this new class of very extended sources in the data will also open a new way of exploring the geometry of the Galactic magnetic field. If a population of sources of this type is discovered, measurements of the directions along which these sources are elongated will trace the direction of the ordered Galactic magnetic field at different locations in the Galactic disk.

Looking for very extended γ-ray sources of this type may also be the only possibility for discovering the elusive sources of the highest-energy ($\gtrsim$PeV) Galactic cosmic rays. The short escape time of these very-high-energy cosmic rays from their sources may preclude the possibility of identifying directly these sources through the interactions of the ~ 10 PeV cosmic rays inside the sources, unless the acceleration event would be observed "live," for example during the next Galactic supernova. The fast spread of ~ 10 PeV cosmic rays through the interstellar medium also reduces the possibility of catching the signal from cosmic ray interactions in the immediate vicinity of the source (for example, in molecular clouds adjacent to the source). The detection of emissions extending on $\gtrsim 10°$-scales and stretching along the ordered Galactic magnetic field may therefore provide a new and more robust way of identifying of the long-sought-after sources of 1–10 PeV Galactic cosmic rays.

---

[1] M. Amenomori, Y. W. Bao, X. J. Bi, D. Chen, T. L. Chen, W. Y. Chen, X. Chen, Y. Chen, Cirennima S. W. Cui, Danzengluobu L. K. Ding et al., Phys. Rev. Lett. **126**, 141101 (2021).

[2] A. U. Abeysekara, A. Albert, R. Alfaro, J. R. A. Camacho, J. C. Arteaga-Velázquez, K. P. Arunbabu, D. Avila Rojas, H. A. Ayala Solares, V. Baghmanyan et al. (HAWC Collaboration), Phys. Rev. Lett. **124**, 021102 (2020).

[3] Z. Cao, F. A. Aharonian, Q. A. Axikegu, L. X. Bai, Y. X. Bai, Y. W. Bao, D. Bastieri, X. J. Bi, Y. J. Bi, H. Cai et al., Nature (London) **594**, 33 (2021).

[4] W. D. Apel, J. C. Arteaga-Velázquez, K. Bekk, M. Bertaina, J. Blümer, H. Bozdog, I. M. Brancus, E. Cantoni, A. Chiavassa, F. Cossavella et al., Astropart. Phys. **47**, 54 (2013).

[5] M. G. Aartsen, M. Ackermann, J. Adams, J. A. Aguilar, M. Ahlers, M. Ahrens, C. Alispach, K. Andeen, T. Anderson, I. Ansseau *et al.*, Phys. Rev. D **100,** 082002 (2019).

[6] T. Sudoh, T. Linden, and D. Hooper, J. Cosmol. Astropart. Phys. 08 (2021) 010.

[7] A. Neronov and D. V. Semikoz, Phys. Rev. D **85,** 083008 (2012).

[8] J. Binney and S. Tremaine, *Galactic Dynamics: Second Edition* (Princeton University Press, Princeton, NJ, 2008).

[9] E. Poggio, R. Drimmel, T. Cantat-Gaudin, P. Ramos, V. Ripepi, E. Zari, R. Andrae, R. Blomme, L. Chemin, G. Clementini *et al.*, Astron. Astrophys. **651,** A104 (2021).

[10] M. J. Reid, K. M. Menten, A. Brunthaler, X. W. Zheng, T. M. Dame, Y. Xu, J. Li, N. Sakai, Y. Wu, K. Immer *et al.*, Astrophys. J. **885,** 131 (2019).

[11] R. Drimmel and D. N. Spergel, Astrophys. J. **556,** 181 (2001).

[12] D. Skowron, J. Skowron, P. Mróz, A. Udalski, P. Pietrukowicz, I. Soszyński, M. Szymański, R. Poleski, S. Kozlowski, K. Ulaczyk *et al.*, Acta Astron. **69,** 305 (2019).

[13] R. Jansson and G. R. Farrar, Astrophys. J. **757,** 14 (2012).

[14] R. Jansson and G. R. Farrar, Astrophys. J. Lett. **761,** L11 (2012).

[15] G. Giacinti, M. Kachelriess, and D. V. Semikoz, J. Cosmol. Astropart. Phys. 07 (2018) 051.

[16] A. Neronov and D. Malyshev, arXiv:1505.07601.

[17] A. Neronov, D. Malyshev, and D. V. Semikoz, Astron. Astrophys. **606,** A22 (2017).

[18] A. Neronov and D. Semikoz, Astron. Astrophys. **633,** A94 (2020).

[19] G. Giacinti, M. Kachelrieß, and D. V. Semikoz, Phys. Rev. D **90,** 041302 (2014).

[20] G. Giacinti, M. Kachelrieß, and D. V. Semikoz, Phys. Rev. D **91,** 083009 (2015).

[21] G. Giacinti, M. Kachelrieß, D. V. Semikoz, and G. Sigl, J. Cosmol. Astropart. Phys. 07 (2012) 031.

[22] M. Kachelrieß, I. V. Moskalenko, and S. Ostapchenko, Comput. Phys. Commun. **245,** 106846 (2019).

[23] S. Koldobskiy, M. Kachelrieß, A. Lskavyan, A. Neronov, S. Ostapchenko, and D. V. Semikoz, Phys. Rev. D **104,** 123027 (2021).

[24] A. Neronov and D. Semikoz, Phys. Rev. D **102,** 043025 (2020).

[25] S. Zhao, R. Zhang, Y. Zhang, and Q. Yuan, Proc. Sci. ICRC2021 (**2021**) 859.

[26] R.-Y. Liu and X.-Y. Wang, Astrophys. J. Lett. **914,** L7 (2021).